JOURNAL OF Applied Polymer SCIENCE

Reinforcement of Biodegradable Poly(butylene succinate) with Low Loadings of Graphene Oxide

Chaoying Wan,[1] Biqiong Chen[2]

[1]Department of Mechanical Engineering, School of Computing, Engineering and Information Science, Northumbria University, Newcastle upon Tyne NE1 8ST, United Kingdom

[2]Department of Materials Science and Engineering, University of Sheffield, Mappin Street, Sheffield S1 3JD, United Kingdom

Correspondence to: B. Chen (E-mail: biqiong.chen@sheffield.ac.uk)

ABSTRACT: The structure and mechanical properties of biodegradable poly(butylene succinate) (PBS)/graphene oxide (GO) composites were investigated. Chemically exfoliated GO nanosheets with an average lateral dimension of 1.50 (±0.15) μm and an average thickness of 1.18 (±0.09) nm were prepared by a modified Hummers method and used for reinforcement of PBS because of its abundant oxygen-containing functional groups. The GO was dispersed as several layers in the PBS matrix through solution-blending and compression-molding methods that were characterized by transmission electron microscopy. The tensile strength, Young's modulus, and fracture energy of PBS were increased by 53, 70, and 100%, respectively, with an incorporation of 2.0 wt % of GO. The stiffness of PBS/GO composites was predicted using the Halpin–Tsai model and considering a two-dimensional random dispersion of GO nanoplatelets in the PBS matrix and the effective volume fraction of the reinforcement. The crystallization temperature and crystallinity of PBS were increased by the addition of GO, indicating that it acts as a nucleating agent to facilitate the crystallization of PBS. The improvement of physical and mechanical properties of biodegradable PBS with the incorporation of low loadings of GO nanoplatelets further expands its industrial uses. © 2012 Wiley Periodicals, Inc. J. Appl. Polym. Sci. 000: 000–000, 2012

KEYWORDS: differential scanning calorimetry; mechanical properties; polymer-matrix composites; stress transfer

Received 23 March 2012; accepted 3 June 2012; published online

DOI: 10.1002/app.38136

INTRODUCTION

Development of biodegradable polymer composites with improved physical, mechanical, optical, thermal, and/or electrical conductivity properties has been regarded as an important direction or solution for global environmental problems caused by plastic wastes.[1] Various investigations[2,3] have been carried out on biodegradable polymers, which are produced from renewable or petroleum resources such as poly(butylene adipate/terephthalate), poly(L-lactic acid), poly(ε-caprolactone) (PCL), poly(ethylene terephthlate/succinate), and poly(butylene succinate) (PBS). As one of aliphatic thermoplastic polyesters, PBS is synthesized through the polycondensation reaction of glycols such as ethylene glycol and 1,4-butanediol, and aliphatic dicarboxylic acids such as succinic acid and adipic acid.[4] It has a range of desirable properties including melt processability, thermal and chemical resistance, and especially natural decomposition by bacteria and fungi.[5] As a semicrystalline polymer (crystallinity 35–45%), PBS has a glass transition temperature of −32°C, a melt temperature of 115°C, similar processibility to that of polyethylene and similar physical properties to those of polyethylene terephthalate.[1] But the mechanical and thermal properties of pristine PBS are not sufficient for various end-use applications. Many efforts have been carried out in modification of PBS to improve its thermal stability and mechanical properties. Various cellulous materials, such as wood flour, rice husk flour, wheat straw, sisal-fiber, and starch, have been applied to reinforce PBS to produce low-cost, low-density, biodegradable and nontoxic composites,[1,6,7] which can be considered as attractive alternatives to conventional plastic materials in particular for injection-molded and disposable packaging products. However, poor dispersion, interfacial adhesion, and processing properties of these cellulous materials filled polymer composites often limit the reinforcement efficiency and practical applications.

Conversion into composites is an effective way of addressing these drawbacks and widening the application of polymers. Various nanoparticles, such as organoclay,[8–10] carbon nanotubes (CNT),[11–13] polysilsesquioxane,[14] and silica[15] have been applied to modify PBS via solution-blending, *in situ* polymerization or melt-compounding methods. It was reported that the storage flexural modulus of PBS was increased by 88% with the

incorporation of 3.0 wt % of multiwalled CNT (MWCNT), and the in-plane electrical conductivity of PBS was increased from 5.8×10^{-9} S cm^{-1} (considered as nonconductive) to 4.4×10^{-3} S cm^{-1}, representing a 10^6-fold improvement.[12] With the assistance of a modifier, *N*,*N*′-dicyclohexylcarbodiimide, the dispersion of MWCNT (3.0 wt %) in the PBS matrix was significantly improved. As a result, the storage modulus and loss modulus of PBS were increased by 120 and 55%, respectively. The surface resistivity of PBS was decreased by 10^9 folds accordingly.[13] A good dispersion of clay nanolayers or silica nanoparticles in PBS was also realized through in situ polymerization process, however, the stiffness and toughness of the final composites were modestly improved.[8,11,15]

Graphene, a single layer of aromatic carbon, has recently been considered as a promising candidate in polymer reinforcement, optical, electrical, and thermal conductive applications due to its intrinsic extraordinary properties.[16–18] With Young's modulus of 1 TPa and ultimate strength of 130 GPa, single-layer graphene is the strongest material ever measured.[16] The theoretical specific surface area of individual graphene sheets is 2630–2965 m^2 g^{-1},[17] and the aspect ratio is up to over 2000,[18] which allows it to be an outstanding reinforcement for polymers. However, to the authors' best knowledge, there is only one recent report on the reinforcement of PBS by chemical reduced graphene oxide (GO).[19] Although the electrical conductivity and thermal stability of the composites were improved by the addition of graphene sheets, the mechanical properties of PBS were mildly improved, that is, improvements of 21 and 24% in tensile strength and storage modulus of PBS were achieved with the addition of 2.0 wt % of graphene. As compared to graphene, GO nanosheets carrying abundant oxygen-containing functional groups are expected to have stronger interfacial interactions with polar polymers, which will lead to more homogeneous dispersion and higher reinforcement efficiency. In this article, using chemically exfoliated GO nanoplatelets as reinforcement, we have investigated the interfacial interaction and reinforcement efficiency of GO on PBS by means of microstructure characterization and micromechanical modeling methods. The reinforcement mechanism of GO on PBS was discussed by quantification of the interphase zone and simulation with the Halpin–Tsai model with consideration of the effective volume fractions of the reinforcing nanofiller.[20,21] The effects of GO on the crystallization temperature (T_c) and crystallinity (X_c) of PBS were studied using differential scanning calorimetry (DSC). The illustration of the relationship between interphase and reinforcement effects of biodegradable PBS/GO composites is expected to provide useful information for the development of environmentally friendly biomedical and packaging products.

EXPERIMENTAL

Materials

PBS with weight-average molecular weight of 1.3×10^5 Da and density of 1.26 g cm^{-3} was purchased from Anqing Hexing Chemicals, Anhui Province, China. Graphite powder with an average particle size of 6 μm was purchased from Sigma–Aldrich. Chemicals including $NaNO_3$, $KMnO_4$, concentrated H_2SO_4, concentrated HCl, 30% H_2O_2 aqueous solution, dimethylformamide (DMF), and chloroform were all analytical grade and purchased from Sigma–Aldrich.

Preparation of PBS/GO Composites

Chemical oxidation of graphite was conducted following a modified Hummers method.[22] The graphite oxide powder obtained was dispersed in DMF under continuous stirring and ultrasonicated for 1 h to obtain GO/DMF dispersion with a concentration of 0.6 wt/vol %. PBS/chloroform solution (10 wt/vol %) was prepared by dissolving PBS in chloroform at 60°C. Then, the obtained polymer solution was mixed with different amounts of GO/DMF (0.6 wt/vol %) dispersions to prepare PBS/GO solutions with GO concentrations of 0, 0.3, 0.5, 1.0, and 2.0 wt % in the composites, respectively. The resultant mixed solutions were kept stirring for 6 h, then cast onto Petri dishes and oven-dried at 60°C until the weights reached constant. The dried composites were further compression molded at 130°C to prepare composite films for mechanical testing.

Characterization

Dispersion of GO in PBS/GO composites was characterized by transmission electron microscopy (TEM; JEOL 2100) at 200 kV. The PBS/GO composite with GO concentration of 1.0 wt % was microtomed into several sections in $\sim$ 80 nm thickness with a diamond knife (Reichert Ultracut). The fracture surface of PBS/GO samples after tensile testing was coated with 10 nm platinum and then observed using field emission scanning electronic microscopy (SEM, Tescan MIRA) at 5 kV. Thermal properties of PBS/GO composites with various GO concentrations were analyzed by DSC (Perkin-Elmer Diamond DSC). The samples were quenched to −60°C with liquid nitrogen first, then heated up to 150°C at a rate of 10°C min^{-1}, held at 150°C for 3 min, cooled down to −60°C at 10°C min^{-1}, and finally heated up to 150°C at 10°C min^{-1}. The melting point (T_m) and heat of fusion (ΔH_m) were evaluated from a maximum position of the endothermic peak and its area on the DSC curves, respectively. The crystallization temperature (T_c) was evaluated from a maximum position of the exothermic peak of the DSC curves. Tensile tests were performed on a Zwick Z005 universal static testing machine (Zwick GmbH, Ulm, Germany) with a 100 N load cell and a crosshead speed of 2 mm min^{-1} in accordance with ASTM D882-10 standard. The average values and standard deviations were determined from testing five specimens of each sample.

RESULTS AND DISCUSSION

Typical tensile stress–strain curves of PBS/GO composites are depicted in Figure 1, and the mechanical properties are summarized in Table I. The stress–strain curve of PBS moved upward with increasing GO concentration, suggesting increases of the strength and stiffness of the PBS. The elongation at break also increased in most cases. When the GO concentration was 2.0 wt %, the tensile strength, Young's modulus, elongation at break, and fracture energy of PBS were increased by 53, 70, 12, and 100%, respectively, which are significantly higher than those of CNT reinforced PBS composites.[11–13] The geometry of the GO nanoplatelets allows them to offer isotropic reinforcement in more than one direction as compared to CNT. The strong

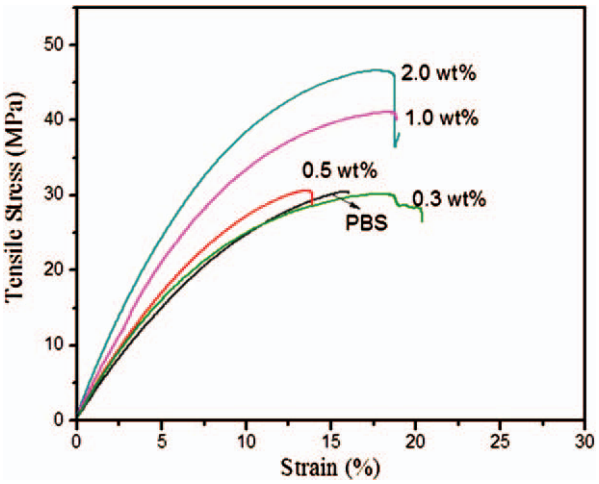

Figure 1. Tensile stress–strain curves of PBS/GO composites with various GO concentrations. [Color figure can be viewed in the online issue, which is available at wileyonlinelibrary.com.]

interfacial interactions between the GO and the PBS matrix originating from the abundant oxygen-containing functional groups on the GO surface and the carboxyl groups of PBS macromolecular chains, as well as the mobility and possible delamination of the GO nanoplatelets under tensile stress[23,24] provide simultaneous improvements in strength, stiffness, ductility, and toughness of the matrix, which will be further discussed subsequently. The slightly lower elongation at break of the PBS/GO (0.5 wt %) composite, compared to the value for the pristine PBS, could be ascribed to measurement error and perhaps also defects in the samples.

The PBS/GO composite films were prepared by solution-casting followed by compression-molding. So, the GO layers were dispersed randomly in two dimensions (2D), that is, the longitudinal and transverse directions in respect to the test direction. The Young's modulus of the composites (E_c) can be expressed as either the longitudinal modulus (E_{11}) or transverse modulus (E_{22}) in the Halpin–Tsai equations [eqs. (1) and (2)].[25]

$$\frac{E_c}{E_m} = \frac{1 + \xi\eta\phi_g}{1 - \eta\phi_g} \tag{1}$$

$$\eta = \frac{(E_g/E_m) - 1}{(E_g/E_m) + \xi} \tag{2}$$

where E_m is Young's modulus of the polymer matrix, E_g is Young's modulus of GO reinforcing filler and is taken as 207.6 GPa given the similarity in the modulus for single or several GO sheets.[26] ξ is the shape factor depending on the filler geometry and loading direction, and $\xi = 2l/3t$ was proposed for E_E calculations for nanoplatelet reinforcement.[27] ϕ_g is the nominal volume fraction of nanoplatelets calculated as 0.18, 0.30, 0.60, and 1.21 vol %, respectively, according to eq. (3):

$$\phi_g = \frac{W_g}{W_g + (\rho_g/\rho_m)(1 - W_g)} \tag{3}$$

where W_g is the weight fraction of GO in the composite, ρ_m and ρ_g are the densities of PBS (1.26 g cm^{-3}) and GO (2.1 g cm^{-3} determined by a pycnometry method in our previous work[28]), respectively.

The E_c values of PBS/GO composites calculated according to eqs. (1) and (2) using nominal volume fractions are shown in Figure 2(a). These values underestimated the experimental data that are in agreement with our previous work.[21,28]

The dispersion state of GO nanoplatelets in the PBS matrix was characterized by TEM. As shown in Figure 2(b), GO nanoplatelets were well dispersed in the polymer matrix when the nanofiller concentration was 1.0 wt %. At a higher magnification [Figure 2(c)], flexible GO nanoplatelets with an average lateral extension $L = 850$ nm and an average thickness $t \approx 16$ nm, giving an aspect ratio $A_f = L/t = 53$, were observed. The average thickness and length of GO stacks in polymer matrix were measured and calculated from over 40 stacks of GO sheets from at least five different TEM images. The chemically exfoliated GO sheets prepared following a modified Hummers method in our work have an average $L = 1.50$ ($\pm$0.15) μm and $t = 1.18$ ($\pm$0.09) nm giving an $A_f = 1271$ as characterized via atomic force microscopy.[21] The significantly reduced A_f value of GO in the PBS/GO composite as compared to its original A_f of 1271 reflects that the GO nanoplatelets are dispersed as several-sheet stacks with an average sheet number of 21 in PBS, based on the average thickness of single GO nanosheets being 0.77 nm determined from X-ray diffraction (XRD) patterns.[21] Therefore, under current processing condition, GO was not fully exfoliated as single nanosheets but dispersed as stacks of nanosheets, and such stacks played the reinforcing role as a unit efficiently on the basis of the mechanical enhancements.

Abundant oxygen-containing functional groups, including carbonyl and carboxyl groups (C═O), hydroxyl groups (O—H),

Table I. Mechanical Properties of PBS/GO Composite Films

GO concentration (wt %)	Young's modulus (GPa)	Ultimate tensile strength (MPa)	Elongation at break (%)	Fracture energy (MJ m^{-3})
0	0.315 ± 0.04	30.5 ± 1.6	15.7 ± 42.2	3.14 ± 0.29
0.3	0.358 ± 0.04	30.4 ± 4.1	18.5 ± 45.3	4.45± 0.36
0.5	0.364 ± 0.10	30.7 ± 3.2	13.8 ± 40.5	2.74 ± 0.29
1.0	0.435 ± 0.10	41.8 ± 4.6	18.5 ± 95.3	5.38 ± 0.52
2.0	0.537 ± 0.10	46.7 ± 5.7	17.6 ± 80.5	6.31 ± 0.35

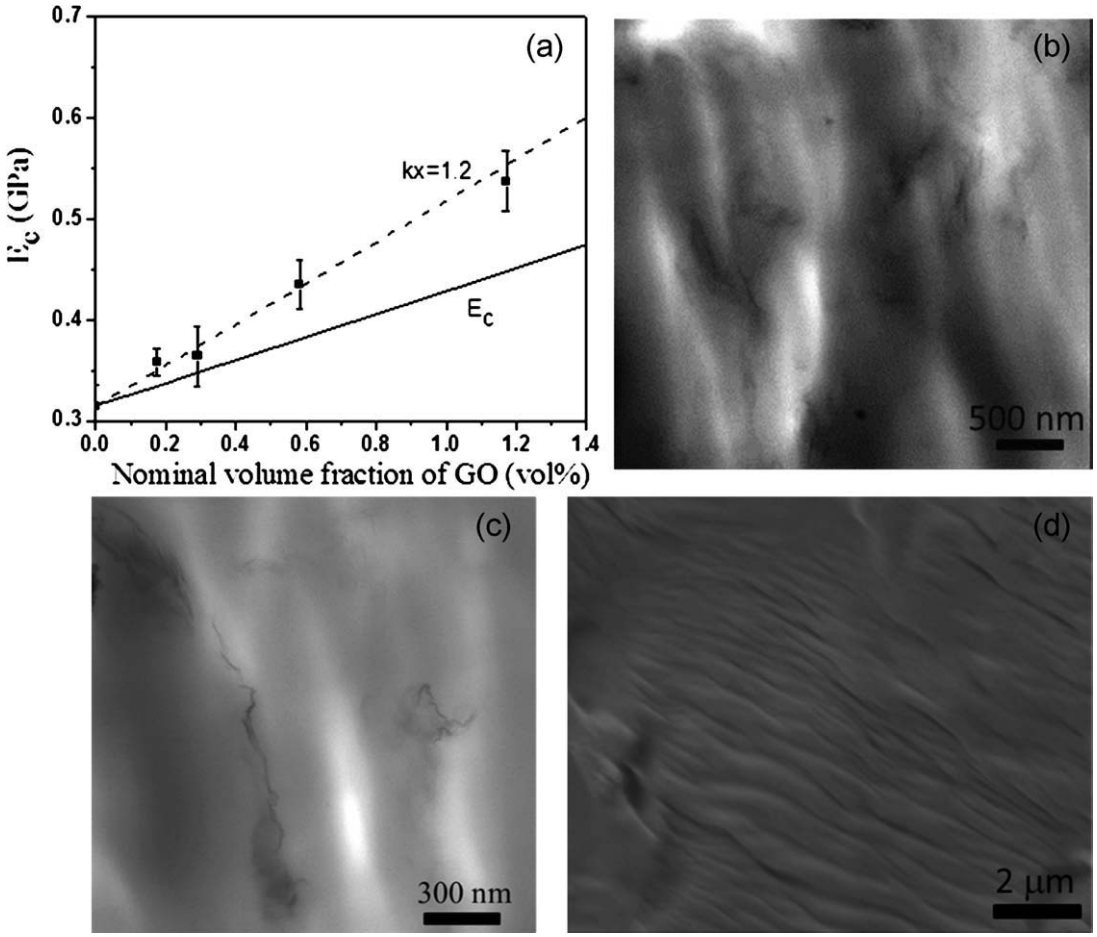

Figure 2. (a) Experimental modulus data for PBS/GO composites and the theoretical values predicted using the Halpin–Tsai model based on the effective volume fractions and nominal volume fractions of GO; (b,c) TEM images of PBS/GO composite with 1.0 wt % GO at different magnifications; and (d) SEM image of the fracture surface of PBS/GO composite with 1.0 wt % GO.

and epoxy ether or peroxide groups (C—O), were detected on the GO surface in our previous work using Fourier transform infrared spectroscopy[29] and X-ray photoelectron spectroscopy.[21] Such functional groups promise strong interfacial interactions with PBS macromolecular chains, so that a substantial amount of polymer chains could adsorb on the GO surface through hydrogen-bonding or electrostatic interactions and form an interphase in between the GO sheets and the PBS matrix. The Halpin–Tsai model assumes that the particle and matrix are linearly elastic, isotropic, and firmly bonded without considering the particle–particle interactions.[25,27,30] The interphase region in polymer composites is generally composed of a layer of crystalline polymer or ordered polymer chains, and its thickness depends on the interactions between the polymer and the nanoparticle as well as the determination method. An interphase form of a semicrystalline polymer layer with $\sim$ 45 nm in thickness was observed by field emission SEM in PCL/GO composites.[31] A direct observation of a $\sim$ 48 nm-thick polymer sheathing in polycarbonate/CNT composites was presented by far-field scanning microscopy.[32] Similarly, a bound rubber layer in $\sim$ 20 nm thickness was visually determined in rubber/carbon black composites by scanning probe microscopy.[33]

To interpret the reinforcement of nanoparticles on polymers, we introduced an effective volume fraction of GO into the Halpin–Tsai model by assuming the layer of adsorbed polymer chains on the GO nanosheet surface has a thickness of xR_g of the polymer, where the effective volume fraction of the reinforcement can be written as eq. (4).[20,21,28]

$$\varphi_g' = \phi_g(1 + kxR_gA_T\rho_g) \tag{4}$$

where k is the fraction of the adsorbed polymer phase (interphase) behaving like the nanofiller. R_g is the radius of gyration of polymer, $R_g = b\sqrt{N/6}$ with N being the number of Kuhn monomers and b being the Kuhn monomer length.[34] x is the coefficient relevant to the thickness of the adsorbed polymer layer and R_g of the polymer. A_T is the specific surface area of the nanofiller.[20] The A_T of GO powder synthesized in our work was measured as 462 $m^2\ g^{-1}$ by B.E.T. surface analysis,[21] but it was reduced to $\sim$ 22 $m^2\ g^{-1}$ due to the aggregation or stacking of GO sheets in polymers by considering the actual number of the GO platelets per stack in the polymer matrix and neglecting the contribution of the side surfaces of the GO platelets. According to our previous work,[20,21,28,29] the mechanical

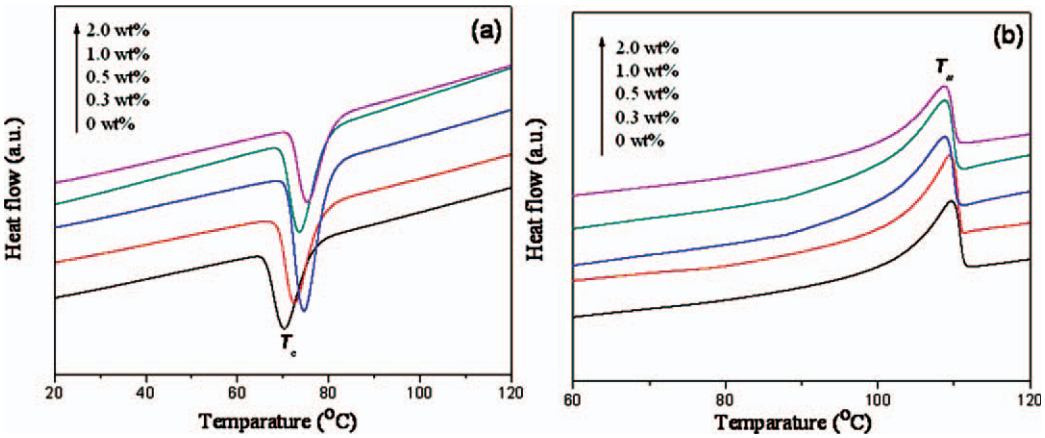

Figure 3. DSC thermograms of PBS/GO composites with various GO concentrations: (a) first cooling curves and (b) second heating curves. [Color figure can be viewed in the online issue, which is available at wileyonlinelibrary.com.]

properties of polymer composites are dependent on the effective volume fraction of the reinforcement, which is greater than the nominal volume fraction of the nanoparticle, because the reinforcement inclusions consisted of inorganic nanoparticles and the adsorbed polymer chains that are considered as a fraction of the nanoparticles due to the lower modulus.

Using the line fitting curve of the experimental data in Figure 2(a), the coefficient *kx* for PBS/GO composites was estimated to be 1.2. This means that the thickness of the "effective interphase zone" that exerts the same modulus as GO stacks of several nanosheets[28] is $1.2R_g$ for the PBS and GO combinations investigated, and it is not simply the thickness of the adsorbed polymer layer like those described earlier.[31–33] This value falls within the typical range of the thickness of the effective interphase zone determined in our previous work for GO and different types of polymers, being $0.12–1.43R_g$.[28] It should be noted that the structure and properties of the interphase between nanoparticles and polymer matrix differ from case to case, which are dependent on various factors including the structure and content of the nanofiller, the structure and molecular weight of the polymer matrix and the determination method. It is interesting to see that the fracture surface of PBS/GO (1.0 wt %) [Figure 2(d)] presented layered structures (which is, however, absent in the surface of the pristine PBS), and the average thickness of each layer is $\sim$ 40 nm. As mentioned earlier, the GO nanoplatelets were dispersed as stacks with an average thickness of 16 nm. The theoretical thickness of the effective interphase zone was $1.2R_g$, which is 14.4 nm (R_g = 12 nm) and is a fraction, *k*, of the thickness of the actual interphase. These imply the total thickness of GO stacks and the actual interphase should be greater than 30.4 nm. Thus, the layer thickness observed in the SEM image agrees well with the micromechanical modeling and TEM results. The absence of bare GO sheets on the fracture surface also confirms the strong bonding between the polymer and GO as previously discussed.

The effect of GO on the crystallization of PBS was investigated using DSC technique, and the DSC results of the first cooling and second heating for PBS/GO composites with various GO concentrations are shown in Figure 3 and Table II. The T_c of PBS was increased with increasing GO concentration, and it was increased by 5°C when the GO concentration was 2.0 wt %. Meanwhile, the heat of fusion (ΔH_m) value of PBS was also increased and the crystallinity (X_c) of PBS was increased accordingly. The result indicates that the GO plays the role of a nucleating agent and promotes the crystallization ability of PBS. The addition of GO has little influence on the T_m of PBS. Similar phenomena were found in GO/PCL composites, in which the T_c was increased by 9°C with incorporation of 2.0 wt % of GO nanoplatelets and the crystal size of PCL became smaller after the addition of GO as observed by polarized light microscopy.[31] This also confirms the nucleating role of GO on the polymer matrix, which is similar to that of CNT or clay on PBS.[8–12] These results suggest the addition of GO into PBS influences its crystallization process and crystallinity in addition to mechanical properties discussed earlier. Again, the lower X_X of PBS/GO (0.5 wt %) could be due to measurement error and/or originate from the nanocomposite preparation process.

CONCLUSIONS

Significant increases in stiffness, strength, and toughness were achieved in biodegradable PBS/GO composites with low loadings of GO nanoplatelets. The tensile strength, Young's modulus, and fracture energy of PBS were increased by 53, 70, and 100%, respectively, with an incorporation of 2.0 wt % of GO, due to strong interfacial interactions between the GO and the

Table II. DSC Results of PBS/GO Composites

GO concentration (wt %)	T_m (°C)	ΔH_m (J g^{-1})	X_c (%)[a]	T_c (°C)
0	110	66.5	60.3	70.3
0.3	110	72.4	65.6	72.6
0.5	109	70.0	63.5	74.6
1.0	109	73.9	67.0	73.7
2.0	109	76.3	69.2	75.4

[a] $X_c = \Delta H_m/(1 - W_g)\Delta H_m^0$, where ΔH_m^0 = 110.3 J g^{-1}, the heat of fusion for 100% crystalline PBS.[6]

PBS matrix and mobility of the GO nanoplatelets under tensile stress. The Halpin–Tsai model was used to predict the stiffness of PBS/GO composites by considering a 2D random dispersion of the GO nanoplatelets in the PBS matrix and the effective volume fraction of the reinforcement. An effective interphase zone that behaves like stacks of GO nanoplatelets was quantified to have a thickness of $1.2R_g$. The addition of GO nanoplatelets into PBS increased its crystallization temperature and crystallinity, indicating that the GO acted as a nucleating agent and facilitated the crystallization of PBS. The GO modified PBS composites with increased physical and mechanical properties will expand the industrial applications of the biodegradable PBS, such as packaging and biomedical applications.

ACKNOWLEDGMENTS

This research was financially supported by a Marie Curie International Incoming Fellowship within the 7th European Community Framework Programme under Grant Agreement No. PIIF-GA-2009-236739.

REFERENCES

1. Smith, R. In Biodegradable Polymers for Industrial Applications; Woodhead Publishing Limited: Cambridge, **2005;** p 24.
2. Garlotta, D. *J. Polym. Environ.* **2001,** *9*, 63.
3. Fujimaki, T. *Polym. Degrad. Stab.* **1998,** *59*, 209.
4. Bahari, K.; Mitomo, H.; Enjoji, T.; Yoshii, F.; Makuuchi, K. *Polym. Degrad. Stab.* **1998,** *62*, 551.
5. Kim, D.Y.; Rhee, Y.H. *Appl. Microbiol. Biotechnol.* **2003,** *61*, 300.
6. Lin, N.; Yu, J.; Chang, P.R.; Li, J.; Huang, J. *Polym. Comp.* **2011,** *32*, 472.
7. Feng, Y.; Shen, H.; Qu, J.; Liu, B.; He, H. L. *Polym. Eng. Sci.* **2011,** *51*, 474.
8. Chen, G. X.; Kim, H. S.; Yoon, J. S. *Polym. Int.* **2007,** *56*, 1159.
9. Chen, G. X.; Yoon.J. S. *J. Polym. Sci. Part B: Polym. Phys.* **2005,** *43*, 817.
10. Ray, S.S.; Okamoto, K.; Okamoto, M. *Macromolecules* **2003,** *36*, 2355.
11. Tan, L.; Chen, Y.; Zhou, W.; Ye, S.; Wei, J. *Polymer* **2011,** *52*, 3587.
12. Ray, S. S.; Vaudreuil, S.; Maazouz, A.; Bousmina, M. J. *Nanosci. Nanotechnol.* **2006,** *6*, 2191.
13. Shih, Y. F.; Chen, L. S.; Jeng, R. J. *Polymer* **2008,** *49*, 4602.
14. Sakuma, T.; Kumagai, A.; Teramoto, N.; Shibata, M. J. *Appl. Polym. Sci.* **2008,** *107*, 2159.
15. Lim, J. S.; Hong, S. M.; Kim, D. K.; Im, S. S. *J. Appl. Polym. Sci.* **2008,** *107*, 3598.
16. Lee, C.; Wei, X.; Kysar, J. W.; Hone, J. *Science* **2008,** *321*, 385.
17. Chae, H. K.; Siberio-Perez, D. Y.; Kim, J.; Go, Y.; Eddaoudi, M.; Matzger, A. J.; O'Keeffe, M.; Yaghi, O. M. *Nature* **2004,** *427*, 523.
18. Stankovich, S.; Dikin, D. A.; Piner, R. D.; Kohlhaas, K. A.; Kleinhammes, A.; Jia, Y. Y.; Wu, Y.; Nguyen, S. T.; Ruoff, R. S. *Carbon* **2007,** *45*, 1558.
19. Wang, X.; Yang, H. Y.; Song, L.; Hu, Y.; Xing, W. Y.; Lu, H. D. *Comp. Sci. Technol.* **2011,** *72*, 1.
20. Chen, B.; Evans, J. R. G. *Macromolecules* **2006,** *39*, 1790.
21. Wan, C.; Frydrych, M.; Chen, B. *Soft Matter* **2011,** *7*, 6159.
22. Hummers, W. S.; Offeman, R. E. J. *Am. Chem. Soc.* **1958,** *80*, 1339.
23. Shah, D.; Maiti, P.; Jiang, D.; Batt, C.; Giannelis, E. *Adv. Mater.* **2005,** *17*, 525.
24. Wan, C.; Zhang, Y.; Zhang, Y. X.; Qiao, X. Y.; Teng, G. M. *J. Polym. Sci. Part B: Polym. Phys.* **2004,** *42*, 286.
25. Halpin, J. C.; Kardos, J. L. *Polym. Eng. Sci.* **1976,** *16*, 344.
26. Suk, J. W.; Piner, R. D.; An, J.; Ruoff, R. S. *ACS Nano* **2010,** *4*, 6557.
27. van Es, M. Polymer-Clay Nanocomposites, Thesis University of Delft. The Netherlands, **2001**, Chapter 3.
28. Wan, C.; Chen, B. *J. Mater. Chem.* **2012,** *22*, 3637.
29. Wan, C.; Chen, B. *Biomed. Mater.* **2011,** *6*, 055010.
30. Hosford, W. F. In Mechanical Behavior of Materials; Cambridge University Press: New York, **2005;** p 39.
31. Cai, D. Y.; Yusoh, K.; Song, M. *Nanotechnology* **2009,** *20*, 085712.
32. Ding, W.; Eitan, A.; Fisher, F. T.; Chen, X.; Dikin, D. A.; Andrews, R.; Brinson, L. C.; Schadler, L. S.; Ruoff, R. S. *Nano Lett.* **2003,** *3*, 1593.
33. Qu, M.; Deng, F.; Kalkhoran, S. M.; Gouldstone, A.; Robisson, A.; Van Vilet, K. J. *Soft Matter* **2011,** *7*, 1066.
34. Rubinstein, M.; Colby, R. H.In Polymer Physics;Oxford University Press:United Kingdom, **2003;** p 63.